Interaction of fast and slow dynamics in endocrine control systems with an application to β-cell dynamics

Yi-Fang Wang[a], Michael Khan[a], Hugo A. van den Berg[b]

[a] *Biological Sciences, University of Warwick, Coventry CV4 7AL UK*
[b] *Mathematics Institute, University of Warwick, Coventry CV4 7AL UK*

Abstract

Endocrine dynamics spans a wide range of time scales, from rapid responses to physiological challenges to with slow responses that adapt the system to the demands placed on it. We outline a non-linear averaging procedure to extract the slower dynamics in a way that accounts properly for the non-linear dynamics of the faster time scale and is applicable to a hierarchy of more than two time scale, although we restrict our discussion to two scales for the sake of clarity. The procedure is exact if the slow time scale is infinitely slow (the dimensionless ε-quantity is the period of the fast time scale fluctuation times an upper bound to the slow time scale rate of change). However, even for an imperfect separation of time scales we find that this construction provides an excellent approximation for the slow-time dynamics at considerably reduced computational cost. Besides the computation advantage, the averaged equation provided a qualitative insight into the interaction of the time scales. We demonstrate the procedure and its advantages by applying the theory to the model described by Tolić et al. (2000; *J. Theor. Biol.*, **207**: 361–375) for ultradian dynamics of the glucose-insulin homeostasis feedback system, extended to include β-cell dynamics. We find that the dynamics of the β-cell mass are dependent not only on the glycemic load (amount of glucose administered to the system), but also on the way this load is applied (i.e. three meals daily versus constant infusion), effects that are lost in the inappropriate methods used by the earlier authors. Furthermore, we find that the loss of the protection against apoptosis conferred by insulin that occurs at elevated levels of insulin has a functional role in keeping the β-cell mass in check without compromising regulatory function. We also find that replenishment of β-cells from a rapidly proliferating pool of cells, as opposed to the slow turn-over which characterises fully differentiated β-cells, is essential to the prevention of type 1 diabetes.

Keywords: Glucose, Insulin, β-cell, Diabetes, Endocrine control system

1. Introduction

Neuroendocrine control systems respond rapidly to physiological challenges while concurrently undergoing adaptation on a much slower time scales (e.g. Schmidt and Thews, 1989; Frayn, 2003). Moreover, an interplay prevails between processes at disparate scales: the slow adaptation is a dependent on the fast events. Such an interplay is a pervasive characteristic of many biological systems.

Email address: hugo@maths.warwick.ac.uk (Hugo A. van den Berg)

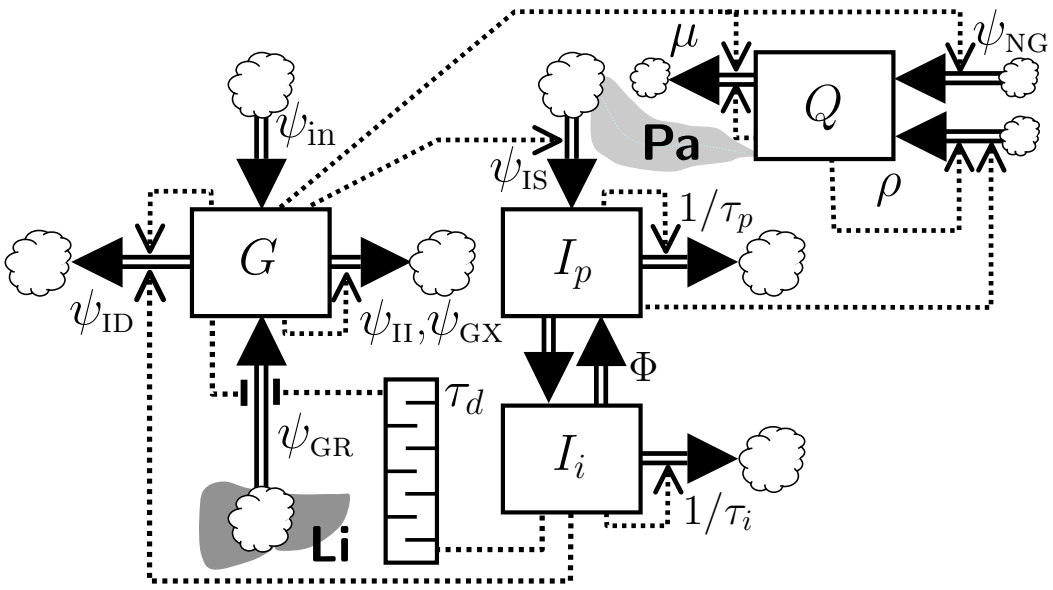

Figure 1: Diagram of the extended Sturis-Tolić model. Squares are state variables, clouds are sources/sinks. Dotted lines indicate functional dependence (arrowheads: positive; blunt ends: negative). A delay line marked τ_d intervenes between I_i and ψ_{GR}. The state variable Q is the relative β-cell mass; with Q fixed at 1, the original Sturis-Tolić model is recovered. **Li**: liver, source of glucose derived from glycogen breakdown. **Pa**: pancreas, site of β-cells which are a source of insulin. See Table 1 for an explanation of the symbols.

As is well known, the dynamics of such systems can be analysed by considering separate and distinct dynamical systems that correspond to the biological system as it operates on two or more "time scales". In such procedures, the approximation usually is exact if the slower component is "infinitely slower" than the faster component (see e.g. Keener and Sneyd, 1998, for examples and applications). On a given time scale, the slower variables are "frozen" and figure as constant parameters, whereas the faster ones can often be treated using a quasi-steady state approximation (up to boundary or transition layers) in which the fast variable is essentially replaced by a function which relates its (fast-time system) equilibrium value to the prevailing values of the slower variables. Similarly, in those cases where the fast-time system does not equilibrate but tends to a periodic solution (e.g., a limit cycle or the stationary response to periodic forcing), intuition would suggest that the fast variables might be replaced by a long-term average. However, this intuition need not be correct. We outline a homogenization method to tackle such problems on two time scales (see Pavliotis and Stuart, 2008, for an introduction to homogenization techniques). The type of system we have in mind describes the dynamics of an organism's physiology (or the relevant part thereof) together with the dynamics of the (neuro)endocrine system that regulates this physiology. We apply the method to a well-established model of the regulation of glucose concentration in the blood plasma, which we extend with a slow component, viz. the dynamics of the mass of endocrine cells. A diagrammatic representation of this system is given in Figure 1.

Introduction to the biological application. Glucose in the blood plasma provides an essential supply of immediately available energy substrate to all tissues of the body (Salway, 1999). Adverse effects ensue when the concentration of glucose in the blood plasma becomes either very low or very high; avoidance of these effects defines a "euglycemic" range of values and, moreover, endocrine control loops operate so as to keep the blood glucose concentration in this range (Watkins, 2003). Whenever the supply of glucose derived from dietary carbohydrate exceeds demand from the tissues, the blood glucose level rises, stimulating the secretion of the hormone insulin, which in turn stimulates the disposition of glucose, either to be taken up as energy substrate rather than fatty acids, or to be stored away as a storage polymer, which is glycogen in liver, muscle, and kidneys, and lipid in adipose tissue (Frayn, 2003). When energy demand outstrips supply, the blood glucose level drops and insulin is not secreted. The resulting drop in the insulin concentration leads to a decrease of insulin-dependent uptake of glucose from the bloodstream as well as an increase of the release of storage-derived glucose from the liver, both of which have the effect of restoring glucose levels. At low levels of glucose, the hormone glucagon is released, which promotes the breakdown of glycogen and fatty acids (Brook and Marshall, 2001). A paracrine interaction between insulin and glucagon secretion has been proposed (Hope et al., 2004). However, inasmuch as glucagon plays a prominent role in humans only when glucose falls significantly below the euglycemic range (Raju and Cryer, 2005), the focus here is on the glucose-insulin feedback loop.

Insulin is a peptide hormone, consisting of two peptide chains linked by disulphide bonds, and produced by the β-cells in the so-called Islets of Langerhans, which are clusters of endocrine cells found scattered throughout the predominantly exocrine pancreas (Brook and Marshall, 2001). The total mass of β-cells changes over time: it continues to do so during adult life and it has become apparent during the past decade that the pathogenesis of both type 1 and type 2 diabetes involves failure to maintain an appropriate β-cell mass (Bonner-Weir, 2000; De León et al., 2003; Lee et al., 2006; Steil et al., 2001). The total mass is the combined result of three processes: proliferation (cell division), apoptosis (programmed cell death), and neogenesis (regeneration from a pool of rapidly dividing cells, which themselves derive from pluripotent stem cells, or possibly de-differentiated β-cells, or alternatively trans-differentiated pancreatic cells); these processes are influenced by the levels of both glucose and insulin (Beith et al., 1998; Bouwens and Rooman, 2005; Dor et al., 2004; Efanova et al., 1998; Johnson and Alejandro, 2008; Lipsett and Finegood, 2002; Rooman et al., 2002; Young et al., 2008). As a result, there is an interplay between the fast, ultradian fluctuations of glucose and insulin and the slower (>days) changes in β-cell mass. This means that we need to consider a fairly realistic, high-dimensional mathematical model on the fast time scale in order to abstract the slow-time dynamics; we choose the model developed by the Lyngby group (see Pattaranit and Van den Berg, 2008, for a review of several comparable models).

2. Theory: time-scale homogenization

The dynamics of a system comprising both the regulated physiology and the associated (neuro)endocrine system can, in many cases, be represented as a dynamical system of the following form:

$$\frac{d}{dt}\mathbf{x} = \mathbf{f}(\mathbf{x}, \mathbf{u}) \tag{1}$$

where $\mathbf{x}$ is the state of the system, $\mathbf{u}$ represents an external input, and $\mathbf{f}$ is the system's dynamics. We assume that the state variables in $\mathbf{x}$ and the input variables in $\mathbf{u}$ have been non-dimensionalised, so that time t is the only unit-bearing quantity remaining. The input $\mathbf{u}(t)$ is assumed to be a

periodic function of time with period T. We now outline a construction that decomposes the original dynamics into two uncoupled systems of lower dynamical dimension. These two systems may be studied independently of one another. The idea is to preserve the way in which features of the dynamics affect the dynamics at the slow time scale, by constructing the slow dynamics as a map that is specific for the fast-scale regime. If this formulation this seems obscure: the application in Section 3 provides examples.

For physiological systems it may naturally be assumed that the rates of change are bounded, that is, for each of the n state variables, there is a finite number ξ_i such that the dynamics of x_i satisfies

$$|f_i(\mathbf{x}, \mathbf{u})| < \xi_i < +\infty \tag{2}$$

as $\mathbf{x}$ and $\mathbf{u}$ range over all physiologically attainable values. Without loss of generality, the state variables can be ordered so that

$$\xi_1 \geq \xi_2 \geq \cdots \geq \xi_n > 0$$

(i.e., fastest first). Scaling of the f_i with respect to the corresponding ξ leads to

$$\frac{d}{dt}\mathbf{x} = \boldsymbol{\xi} \cdot \mathbf{f}^*(\mathbf{x}, \mathbf{u}) \tag{3}$$

where $\boldsymbol{\xi}$ is a diagonal matrix with the ξ_i on its main diagonal and f_i^* is a dimensionless quantity satisfying $|f^*| \leq 1$. We are interested in the case where some variables are "rapid" (i.e. oscillate on a time scale of order T) and others are "slow". That is to say, we consider the case where $\xi_1 \geq T^{-1} \gg \xi_n$ and we assume that there exists an $\nu \leq n$ such that $\xi_i T$ is a small parameter (i.e., $\xi_i T \ll 1$) for $\nu \leq i \leq n$. Anticipating the separation of time scales, we write

$$\mathbf{x}(t) = \mathbf{x}^{[0]}(\varphi(t), \tau(t)) + \mathbf{x}^{[1]}(\tau(t)) \tag{4}$$

where the fast component $\mathbf{x}^{[0]}$ depends on a fast time φ and a slow time τ, whereas the slow component $\mathbf{x}^{[1]}$ depends on slow time τ only. These two times are defined as follows:

$$\varphi = \frac{t}{T} - \left\lfloor \frac{t}{T} \right\rfloor \tag{5}$$

$$\tau = \xi_\nu T \left\lfloor \frac{t}{T} \right\rfloor \tag{6}$$

where $\lfloor x \rfloor$ denotes the largest integer smaller than or equal to x. The input is similarly decomposed;

$$\mathbf{u}(t) = \mathbf{u}^{[0]}(\varphi(t), \tau(t)) + \mathbf{u}^{[1]}(\tau(t)) \; . \tag{7}$$

Let us write

$$\frac{\partial}{\partial \varphi}\mathbf{x}^{[0]} = T\boldsymbol{\xi} \cdot \mathbf{f}^*(\mathbf{x}^{[0]}, \mathbf{u}^{[0]}; \mathbf{x}^{[1]}, \mathbf{u}^{[1]}) \tag{8}$$

for $\varphi \in [0, 1)$. To follow the fast dynamics, equation (8) is integrated from $\varphi = 0$ to $\varphi = 1^-$ subject to initial condition $\mathbf{x}^{[0]} = \mathbf{0}$ at $\varphi = 0$. Now define the following variation: for $\eta \leq \xi_\nu T$ and $i = \nu, \ldots, n$:

$$\delta x_i^{[1]}(\tau, \eta) = T\xi_i \int_0^{\eta/(\xi_\nu T)} f_i^*(\mathbf{x}^{[0]}, \mathbf{u}^{[0]}; \mathbf{x}^{[1]}, \mathbf{u}^{[1]}) d\varphi \tag{9}$$

(this variation may be regarded as a total differential *sensu* Protter and Morrey, 1970, p. 724). Dividing equation (9) by η and specifying for $\eta = \xi_\nu T$, this becomes:

$$\frac{\delta x_i^{[1]}(\tau,\eta)}{\xi_\nu T} = \frac{\xi_i}{\xi_\nu}\int_0^1 f_i^*(\mathbf{x}^{[0]},\mathbf{u}^{[0]};\mathbf{x}^{[1]},\mathbf{u}^{[1]})d\varphi \tag{10}$$

for $i = 1,\ldots,n$. In the limit $\xi_\nu T \to 0$, the following expressions are exact:

$$\frac{d}{d\varphi}x_i^{[0]} = T\xi_i f_i^*(\mathbf{x}^{[0]},\mathbf{u}^{[0]};\mathbf{x}^{[1]},\mathbf{u}^{[1]}) \quad \text{for } i = 1,\ldots\nu-1 \tag{11}$$

$$\frac{d}{d\tau}x_i^{[1]} = \frac{\xi_i}{\xi_\nu}\int_0^1 f_i^*(\mathbf{x}^{[0]},\mathbf{u}^{[0]};\mathbf{x}^{[1]},\mathbf{u}^{[1]})d\varphi \quad \text{for } i = \nu,\ldots n \tag{12}$$

where for $i \geq \nu$ we have $x_i^{[0]} \equiv 0$, τ now denotes the argument of the $\mathbb{R} \mapsto \mathbb{R}$ function $x_i^{[1]}(\cdot)$, and the operator $\partial/\partial\varphi$ has been replaced by $d/d\varphi$ without impunity since φ is restricted to the interval $[0,1)$. If we let $\mathbf{x}_{\nu+}^{[1]} = (x_\nu^{[1]},\ldots,x_n^{[1]})$ then for $i < \nu$ we have $x_i^{[1]} = X_i(\mathbf{x}_{\nu+}^{[1]})$, where $(X_1(\mathbf{x}_{\nu+}^{[1]}),\ldots,X_{\nu-1}(\mathbf{x}_{\nu+}^{[1]}))$ is a parametrical representation of the slow manifold of the dynamics of the system (or a branch of this manifold). The fast variables $x_1,\ldots,x_{\nu-1}$ move close to through a forced limit cycle of period T (and exactly so in the limit $\xi_\nu T \to 0$). The slow manifold can and generally will be varying in slow time τ. It may be desirable to have the slow variable represent a cycle average, rather than the start-of-cycle value which depends on the arbitrary assignment of phase value 0; this is not problematic but would render the notation somewhat more cumbersome and less perspicacious.

3. Calculation: application to the regulation of the glucose concentration in the blood plasma

We apply time-scale homogenization to glycemic homeostasis, which is representative of a well-studied and important physiological system in which fast (regulatory) and slow (adaptive) responses interact in a way that is essential to the system's operation, both in health and disease.

3.1. The extended Sturis–Tolić model

The model for glucose dynamics as originally proposed by Sturis et al. (1991) and subsequently further developed by Tolić et al. (2000) is depicted diagrammatically in Figure 1 and is described

by the following system of ordinary differential equations:

$$\frac{dG}{dt} = \psi_{\text{in}}(t) - \psi_{\text{II}}(G) - \psi_{\text{ID}}(G, I_i) + \psi_{\text{GR}}(G, w_3) - \psi_{\text{GX}}(G) \tag{13}$$

$$\frac{dI_p}{dt} = Q\psi_{\text{IS}}(G) - \Phi\left(\frac{I_p}{V_p} - \frac{I_i}{V_i}\right) - \frac{I_p}{\tau_p} \tag{14}$$

$$\frac{dI_i}{dt} = \Phi\left(\frac{I_p}{V_p} - \frac{I_i}{V_i}\right) - \frac{I_i}{\tau_i} \tag{15}$$

$$\frac{dw_1}{dt} = \frac{3(I_p - w_1)}{\tau_d} \tag{16}$$

$$\frac{dw_2}{dt} = \frac{3(w_1 - w_2)}{\tau_d} \tag{17}$$

$$\frac{dw_3}{dt} = \frac{3(w_2 - w_3)}{\tau_d} \tag{18}$$

$$\frac{dQ}{dt} = (\rho(I_p) - \mu(G))\, Q(t) + \psi_{\text{NG}}(G) \tag{19}$$

where we have adapted the notation slightly to facilitate cross-referencing. In the model, the state variable $G(t)$ denotes the blood plasma content of glucose whereas $I_p(t)$ denotes the blood plasma content of insulin (so that G/V_g and I_p/V_p are plasma concentrations) and $I_i(t)$ is the amount of insulin in the interstitial spaces of the body tissues. Furthermore, $w_1(t)$, $w_2(t)$, and $w_3(t)$ are auxiliary state variables that mimic a delay of duration τ_d in the release of glucose from hepatic glycogen stores, in response to I_p (see Pattaranit and Van den Berg, 2008, for a more detailed explanation); and $Q(t)$ is the β-cell mass, which is a slow state variable presently added to the original model. The input is the forcing function $\psi_{\text{in}}(t)$, which represents the flux of glucose into the blood stream from external sources. The parameter Φ represents the diffusive exchange of insulin between blood and interstitial space; V_p and V_i are the distribution volumes of blood plasma and interstitial space, respectively, for insulin. The parameter τ_p represents the mean life time of an insulin molecule in the blood plasma, whereas τ_i represents the mean life time of an insulin molecule in the interstitial space. These dependencies are modelled in the Sturis–Tolić model by means of plausible, but empirical functional relationships, which are listed in Appendix A.

As indicated in Figure 1, there are a number of rates and fluxes that depend in various different ways on the state variables. Glucose-uptake by the tissue depends on the plasma glucose level only in the case of insulin-independent uptake (ψ_{II}), but also on the plasma insulin level in the case of insulin-dependent glucose uptake (ψ_{id}). When glucose levels become very high, the kidneys begin to excrete glucose; this flux is indicated as ψ_{GX}. Two fluxes contribute to increases of plasma glucose: these are the input from the food (or glucose administered by an injection or infusion), denoted as ψ_{in}, which is treated as a forcing function in the present model, and the second flux is glucose secreted by the liver; this glucose release flux ψ_{GR} is also dependent on both plasma glucose and plasma insulin. Glucose stimulates the secretion of insulin, and thus the insulin secretion ψ_{IS} is glucose-dependent.

The model has been extended here with the dynamics of the β-cell mass, which involves three processes: β-cell proliferation, whose specific rate ρ is assumed to depend on plasma insulin; β-cell death, occurring at a specific rate μ that depends on both plasma glucose and insulin, and a neogenesis flux ψ_{NG} which also depends on both plasma glucose and insulin. Empirical formulas for these dependencies, as well as a justification, is given in Appendices A and B. Inasmuch as the

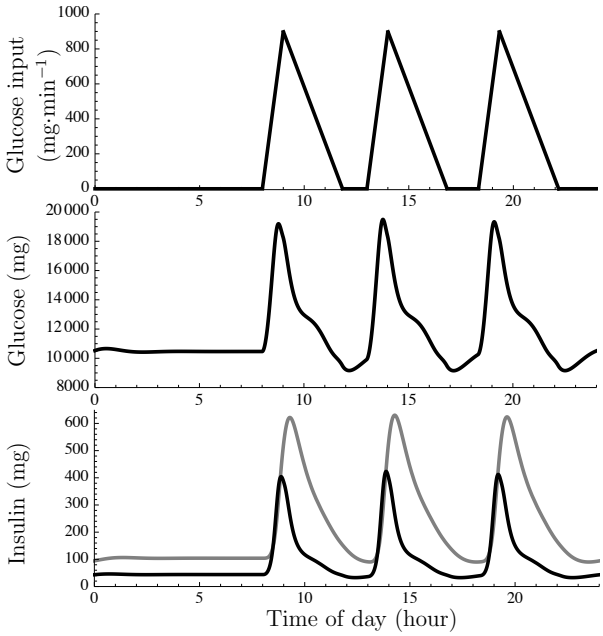

Figure 2: Reference cycle. Top: glucose input; middle: plasma glucose content; bottom: plasma (black line) and interstitial space (grey line) insulin content.

contribution of neogenesis remains to be fully elucidated and may be considered controversial, we shall analyse the model first on the assumption that this term is absent.

The glucose input $\psi_{\rm in}(t)$ can assume various forms. It may be set of a constant value, as can be arranged under experimental conditions where glucose is administered by means of an infusion, or it may be time-varying. If $\psi_{\rm in}$ is set to a constant value, ultradian oscillations may become prominent feature of the dynamics, as shown by Tolić et al. (2000). Here we choose as standard reference a periodic function with a period of 24 hours and three "meal peaks" in every day, as shown in the top panel of Figure 2. Under this particular input, the system settles on a stationary forced cycle within a few days, also shown in Figure 2.

3.2. Analysis without neogenesis of β-cells

To analyse the dynamics in the absence of neogenesis, we set $\widehat{\psi}_{\rm NG} = 0$. It will emerge that the resulting β-cell dynamics is very slow on this assumption, which can be taken as indirect evidence that neogenesis is an important factor in rapid (i.e., hours/days rather than months or years) adaptation, provided we accept the parameter values taken from the literature.

Following the method outlined in Section 2, the steps are to render the system dimensionless, except for time, determine the maximum absolute rates (the ξs), and to rank the scaled variables according to these rates. Choosing 10 g as the reference value for glucose and 44 mU as the reference value for insulin, we find the following ranking (ξs all in $\rm min^{-1}$; Q is already dimensionless):

$x_1 = I_p/I_{\rm ref}$	$x_2 = G/G_{\rm ref}$	$x_3 = I_i/I_{\rm ref}$	$x_4 = w_1/I_{\rm ref}$	$x_5 = w_2/I_{\rm ref}$	$x_6 = w_3/I_{\rm ref}$	$x_7 = Q$
$\xi_1 = 4.8$	$\xi_2 = 0.11$	$\xi_3 = 0.066$	$\xi_4 = 0.028$	$\xi_5 = 0.028$	$\xi_6 = 0.028$	$\xi_7 = 8.7 \times 10^{-7}$

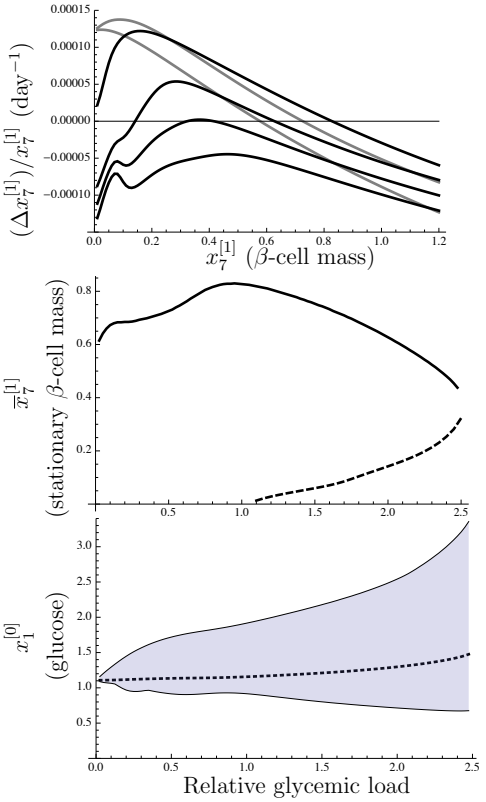

Figure 3: Dynamics of β-cell mass on the slow time scale. Top: relative daily change of β-cell mass, for various glycemic loads (black curves, from top to bottom: 1, 2, 2.5, and 3 times the reference input; grey curves, from top to bottom: 0.5 and 0 times the reference input). Middle: fixed point of the β-cell dynamics as a function of the relative glycemic load (solid line: stable branch; dashed line: unstable branch). Bottom: fast-time scale glucose stationary cycle characteristics (dotted line: average value; bottom and top of filled region: minimum and maximum values).

A time-scale separation at $\nu = 7$ is apparent, with small parameter $\xi_\nu T = 8.7 \times 10^{-7}$ min$^{-1} \times (24 \times 60$ min$) = 0.00125$; a unit of slow time τ thus corresponding to 800 days.

The theory of Section 2 now prescribes that the dynamics in slow time for $x_7^{[1]}$ is derived using equation 12, whereas the variables $x_1^{[1]}, \ldots, x_6^{[1]}$ are to be obtained as functions of $x_7^{[1]}$ on the basis of the slow-manifold condition, which corresponds to the stationary forced cycle in fast time when $x_7^{[1]}$ is held at a fixed value. These relations can be obtained numerically without trouble: results are shown in Figure 3. Since the reference cycle corresponds to a fairly high glycemic load, higher loads may be regarded as hyperglycemic. At such loads, the dynamics of the β-cell mass has two fixed points: a lower unstable one and a higher stable point. The existence of the unstable fixed point, referred to as a "pathological fixed point" by Topp et al. (2000), indicates that catastrophic involution of β-cell mass will occur when x_7 becomes lower than this equilibrium value. It will then decay to zero: the loss of β-cells leads to further hyperglycemia and lower insulinemia, which leads to further β-cell losses (Topp et al., 2000). Such a process may underlie non-autoimmune diabetes

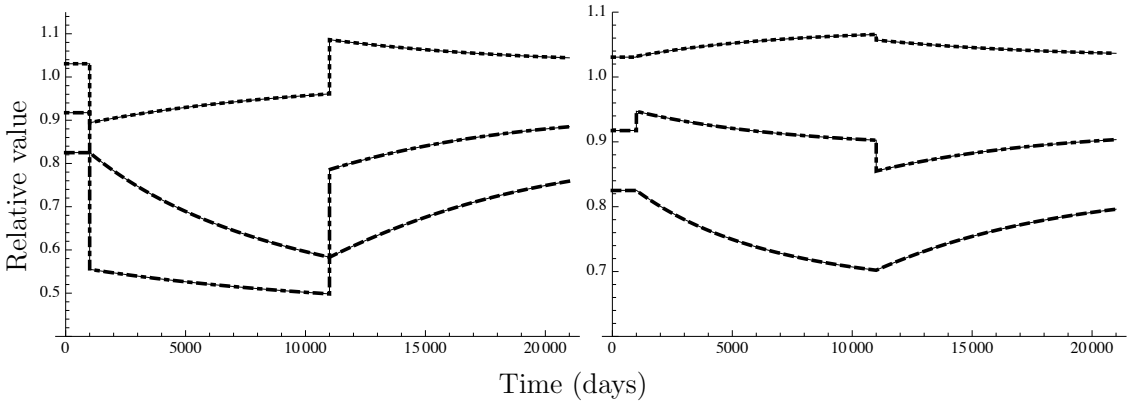

Figure 4: Simulations of overfeeding (left) and (underfeeding) right. On day 1000, the glycemic load is changed to 2.5 (left) or 0.1 (right) normal; on day 11,000 the load is restored to the normal value. Dotted line: slow glucose; dot-dashed line: slow plasma insulin; dashed line: slow β-cell mass. Thin lines show the results of a direct simulation of the 7-dimensional system. ("Relative value" refers to scaling by G_{ref} and I_{ref}, as explained in the text; $Q = x_7 = 1$ corresponds to the stationary value of β-cell mass if the standard-cycle glycemic load were administered at a constant rate; stationary values can be read off from Figure 3.)

mellitus, as described by Imagawa et al. (2000).

As the glycemic load increases, these two fixed points move together and collide. At even higher glycemic loads, the globally attracting point is the trivial equilibrium $Q = 0$, that is, zero β-cell mass. The decrease in the stable equilibrium value with increasing glycemic load is due to an increased β-cell death rate at such high loads, both as a result of higher glucose toxicity (Efanova et al., 1998), and of increased susceptibility to apoptosis at higher insulin levels (Johnson and Alejandro, 2008); the latter authors describe this situation as a "sweet spot" for insulin in the high pico-molar range, which corresponds to order 1 levels in the scaled system.

As might be expected from the strong separation of time scales, the approximation for the slow-time scale dynamics is excellent. Figure 4 compares the dynamics according to the approximation (which is simple and 1-dimensional) to the dynamics of the original, 7-dimensional, system, in an overfeeding and an underfeeding simulation. The results are indistinguishable: thus, the long-term dynamics is well-captured by the approximation. The full system was numerically integrated in fast time using an explicit Runge-Kutta method of order 2(1), which is the *Mathematica* default method (Sofroniou and Spaletta, 2004). The slow system was evaluated using Euler-forward with a step size of one day, giving virtually the same result at less than a thousandth of the computational cost (run time; excluding the one-time cost of establishing the dynamics of x_7, which costs about 1% of the full-system's run time).

In formulating a mathematical model for the long-term dynamics of the β-cell mass, it is tempting, although incorrect, to represent the glycemic load as a constant that represents the average of the daily cycle (e.g., Topp et al., 2000; De Winter et al., 2006; Ribbing et al., 2010). However, the dynamics of $x_7^{[1]}$ in slow time τ do in fact depend critically on the "temporal fine structure" of glucose uptake on the fast time scale t, through the integration in equation (12). Such dependence is neglected by an approach that replaces glucose uptake by its short-term average. This becomes readily apparent when we consider the case where the glycemic load is assimilated as a constant

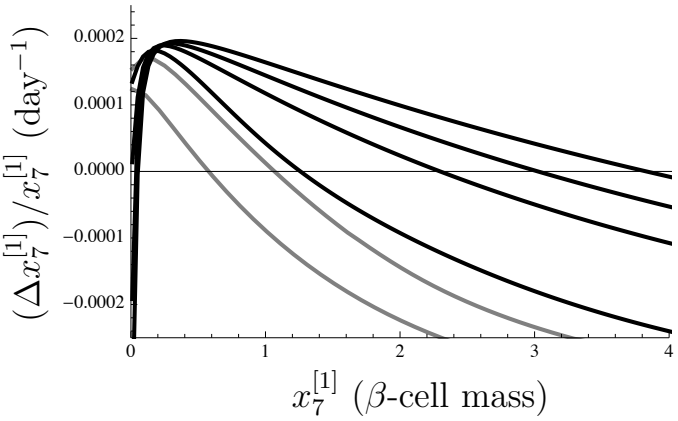

Figure 5: Dynamics of β-cell mass on the slow time scale: relative daily change of β-cell mass, for various glycemic loads, administered as a constant infusion (black curves, from left to right: 1, 2, 2.5, and 3 times the reference input; grey curves, from left to right: 0 and 0.5 times the reference input).

infusion (set to zero for the first 30 minutes after midnight, to enforce a 24-hour cycle) instead of a daily 3-meal cycle. It is found that the long-term dynamics of the β-cell mass is strikingly different: the "pathological fixed point" remains very close to zero and the system achieves near-perfect regulation of the average glucose level even at a hyperglycemic load that is 4 time higher than normal, as shown in Figure 5. Comparison with the case $\iota_{\mathrm{AI}} \to \infty$ (not shown) shows that decrease of insulin's potency in inhibiting apoptosis at high levels is responsible for keeping the β-mass in check without compromising the ability to regulate: for $\iota_{\mathrm{AI}} \to \infty$, the fixed point of x_7 increases sharply with load, even though normalisation of glucose levels is already achieved at x_7-values comparable to those indicated in Figure 5.

3.3. Extended model with neogenesis of β-cells

The response dynamics shown in Figure 4 is very slow. An example of such sluggish dynamics is shown in Figure 6: if 80% of the β-cell mass is destroyed, it takes about 50 years to recover. This means that the subject will be effectively diabetic for much of his or her lifetime; the baseline turn-over dynamics of β-cells is too sluggish to respond adequately to such challenges. However, in reality, recovery from such damage is accomplished within a few weeks' time (Bouwens and Rooman, 2005). It has been proposed that the slowly proliferating β-cell pool may, under certain conditions, be replenished by differentiation of cells from a more quickly proliferating pool of progenitor cells (De León et al., 2003; Rooman et al., 2002) that is phenotypically distinct from the differentiated β-cells themselves (Ackermann Misfeldt et al., 2008). A competing hypothesis is that β-cells themselves are capable of rapid proliferation (Dor et al., 2004; Lee et al., 2006; Nir et al., 2007). The two hypotheses may be reconciled if the rapidly proliferating pool of cells is derived (by a process akin to dedifferentiation) from adult β-cells, since such cells are readily driven back into cell cycle by activation of the proto-oncogene c-myc (Pelengaris et al., 2002). Here, the pool of proliferators will be treated as a source term, an approach compatible with either point of view. We shall refer, for the sake of clarity, to the proliferator pool as "progenitors", with the caveat noted above.

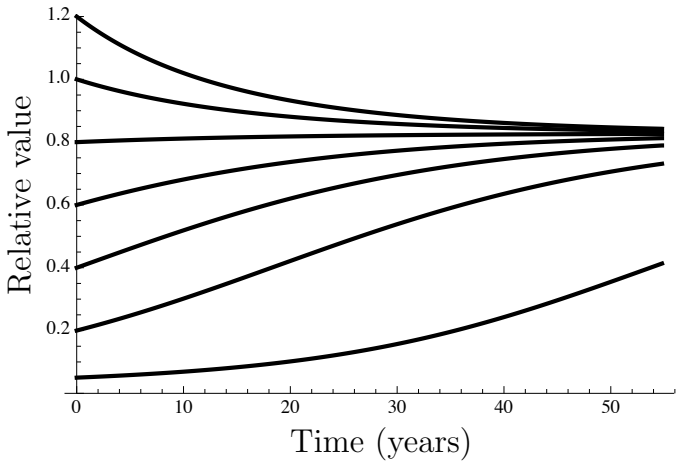

Figure 6: Dynamics of β-cell mass on the slow time scale: recovery to normal values after addition or destruction of β-cells at time $t = 0$. ("Relative value" has the meaning explained in the caption for Figure 4.)

We propose to describe the neogenesis of β-cells from progenitor cells by the following equation:

$$\psi_{\mathrm{NG}}(G) = \widehat{\psi}_{\mathrm{NG}} \left(1 + \exp\left\{\alpha_{\mathrm{NG,g}} \left(1 - \frac{G/V_g}{\gamma_{\mathrm{NG}}}\right)\right\}\right)^{-1} \left(1 + \exp\left\{\alpha_{\mathrm{NG,i}} \left(1 - \frac{I_i/V_g}{\iota_{\mathrm{NG}}}\right)\right\}\right)^{-1} \tag{20}$$

with positive parameters $\widehat{\psi}_{\mathrm{NG}}$, $\alpha_{\mathrm{NG,g}}$, $\alpha_{\mathrm{NG,i}}$, ι_{NG}, and γ_{NG}. This equation is built from the same generic sigmoid building blocks used in the orginal model, to represent graded responses to the relevant stimuli. The key assumption is that neogenesis is driven by prolonged hyperglycemia (Lipsett and Finegood, 2002) in conjunction with elevated insulin levels (Grossman et al., 2010). It may be observed that the right-hand side of equation (20) behaves like a soft AND-gate: the flux ψ_{NG} is large when both glucose and insulin levels are elevated. Prolonged concurrence of high glucose and insulin levels may be associated with insufficiency, so it would make teleological sense, in a manner of speaking, to control β-cell mass compensation in this manner. From a mechanistic point of view, it is known that the pathway regulating rapid β-cell proliferation can act like an AND-gate. Specifically, the proto-oncogene gene c-myc, which encodes the transcription factor c-Myc, which stimulates proliferation as well as susceptibility to apoptosis (Pelengaris and Khan, 2003) such that the net effect is loss of β-cells unless an anti-apoptotic co-signal is present (Pelengaris et al., 2002). Expression of c-Myc is induced by glucose (Jonas et al., 2001) whereas insulin induces an anti-apoptotic signal (Johnson et al., 2006). Thus, whereas glucose alone induces a net loss of β-cells (Van de Casteele et al., 2003), the simultaneous presence of glucose and insulin would stimulate rapid proliferation, possibly via rapid (partial) dedifferentiation of existing adult β-cells to the proliferative phenotype. It has been suggested that this dual proliferation/apoptosis pathway acting via c-myc acts as a fail-safe that defaults to β-cell loss unless both glucose and insulin are elevated (Pelengaris and Khan, 2003).

The action of glucose is indirect and thought to be via glucagon-like peptide 1 (GLP-1; De León et al., 2003), an incretin and cytokine which is secreted by enteroendocrine L-cells. Since the half-life of GLP-1 is extremely short (Mentlein et al., 1993), an instantaneous functional dependence

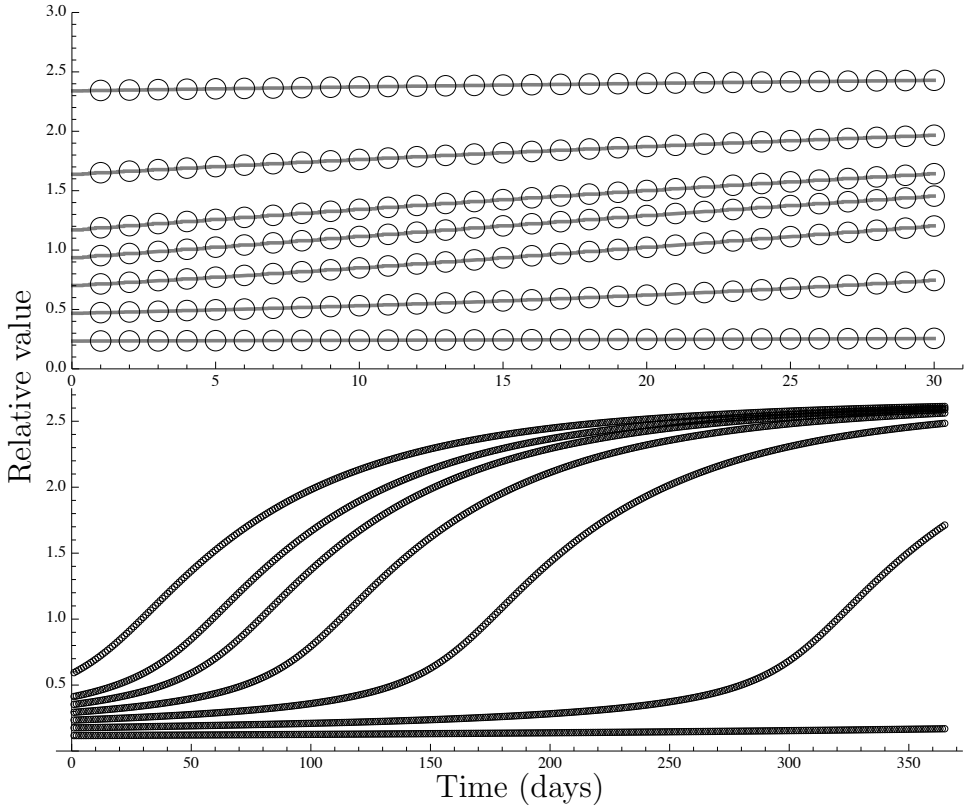

Figure 7: Model with neogenesis: recovery to normal values after addition or destruction of β-cells at time $t = 0$ Gray curves: direct simulation; circles: approximation according to slow-time approximation. Top panel: recovery over a month; bottom panel: recovery over a year. ("Relative value" has the meaning explained in the caption for Figure 4, but the normal stationary value is now different since the dynamics includes neogenesis.)

on G/V_p appears warranted. In principle, ψ_{NG} should also depend on, and be limited by, the amount of progenitor cells present in the pancreas; in the present model, this pool is assumed to be non-limiting and is thought of as an unlimited source.

When neogenesis is included in the model, recovery from partial ablation of β-cell mass is much more rapid and in keeping with the various values quoted in the literature (recovery in a 1 to 5 week period; see Bouwens and Rooman, 2005, for a review of the experimental data), as shown in Figure 7. The slow-time approximation is still excellent, despite the fact that time-scale separation is now up to two orders of magnitude worse due to the rapid β-cell expansion that occurs when the β-cell mass is too low. The relationship between $\frac{d}{d\tau}x_7$ and x_7 remains qualitatively the same, except that the lower, unstable fixed point (the pathological fixed point) is now very low and the positive rate of change that prevails when x_7 lies in between the fixed points is now several orders of magnitude larger.

If too much of the β-cell mass is destroyed, recovery takes disproportionally longer, as shown in the bottom panel of Figure 7: when more than $\sim 80\%$ of the β-cells are destroyed, recovery takes

the best part of a year, which implies the subject is diabetic for a number of months until recovery occurs.

Type 1 diabetes is an illness due to autoimmunity directed against β-cells (Watkins, 2003). The simulations in Figure 7 suggest that there is a critical level of ablation at which recovery becomes very much slower. If the progenitor cells do not express the insulin-derived antigen, or do so in sufficiently low levels to escape immune attack, the progression to type 1 diabetes is a matter of ψ_{NG} being unable to compensate for the losses, leading to a net diminishment of β-cell mass until the critical depletion level is reached. If the progenitor cells are also susceptible to immune attack, the rate of recovery will be further compromised and the rate at which the β-cell mass descends to the critical level may be accelerated.

4. Discussion

The interplay between the glycemic homeostasis feedback loop, which operates on the ultradian time scale, and the adaptive changes in β-cell mass, which happen on a days-to-months time scale, is a typical feature of endocrinological and neuroendocrinological regulation, where a slower adaptive feedback loop is superimposed on a more rapid feedback loop, the latter directly involved with a physiological system, with the former regulating the level of activity in some manner, e.g. by controlling rates of transcription, translation, electrical activity (secretion), or, as in the present example, number of endocrine cells (Brook and Marshall, 2001). Moreover, the dynamics of such systems usually exhibits a strongly non-linear character (Keener and Sneyd, 1998), which means that small variations in the precise time courses of the fast processes (the temporal fine structure) can have a profound effect on the rates of change of the slow processes. Time-scale separation can be a powerful tool to abstract a low-dimensional dynamical system modelling the slow adaptation process, which is considerably more easy to analyse and visualise. In the present case, a 7-dimensional dynamics is reduced to 1-dimensional dynamics, which is straightforward to analyse; indeed, as Figure 3 shows, in qualitative terms the system is much like logistic growth with an Allee effect.

When equation (12) is evaluated (in most cases this needs to be done numerically), the causal relationships may be obscured somewhat. For instance, in the present model, the rate of change of the β-mass is dependent, in the direct, mechanistic sense of the word, on glucose and insulin, as the model's equations make explicit. However, the time courses of glucose and insulin depend on the prevailing β-cell mass, together with the input ψ_{in}, and as a result, in slow time, the rate of change of the β-cell mass depends on the β-cell mass itself plus the input waveform, i.e., the rate of change in slow time is a *functional* of the input $\psi_{\mathrm{in}}(t)$, as is clear from the integration over the fast-time scale cycle in equation (12). In this way, the temporal fine structure is taken into account, in analogy to similar spatial homogenisation procedures (see Keener and Sneyd, 1998, and Holmes, 1995).

The assumption in this paper has been that rapid compensation in β-cell mass is driven by proliferation, based on the observation that β-cells can be driven back into cell cycle by activation of c-myc (Pelengaris et al., 2002) and data on recovery from partial pancreatomy and hyperglycemic challenge (Bouwens and Rooman, 2005). However, it is also possible that β-cells respond by adjusting the amount of hormone-producting machinery per cell (and, concomitantly, cell volume) and that data concerning short-term changes in numbers of β-cells are distorted by the fact that temporarily depleted cells (degranulated cells) are spuriously not counted as β-cells (Akirav et al., 2008). The relative importance of such non-proliferative adaptation, which possibly depends on

the time scales and extend of challenge at hand, remains to be elucidated in detail; whereas hypertrophy was held to be the main mechanism for increases in β-cell mass in man until the last decade (Nielsen et al., 1999; Weir et al., 2001), recent years have seen a change in emphasis towards proliferation and neogenesis (Bouwens and Rooman, 2005; Lingohr et al., 2002; Pelengaris et al., 2002).

In the model considered here, all but one of the state variables was fast. The Sturis–Tolić model can be extended with further slow variables. One such variable might be the insulin sensitivity of the body's tissues, which plays a major role in the etiology of type 2 diabetes (Salway, 1999). However, a more precise characterisation of the process we have referred to as neogenesis is essential to make progress: in particular, the maximum rate at which this pool can proliferate, as well as the rates at which it is replenished (which may depend on the sources: β-cells are transdifferentiated pancreatic cells) are likely to be critical to the ability of neogenesis to furnish the amount of new β-cells required. The present paper has shown that the pathological fixed point, first noted and so termed by Topp et al. (2000), becomes a prominent factor only when neogenesis is impaired, and, moreover, that this pathological fixed point has a value that is dependent on the diel time course of the rate at which glucose is administered to the system. Whereas mathematical modelling can never replace the experiments that elucidate these processes, it can help to characterise the functional consequences of these findings along the lines outlined in the present paper.

Acknowledgements. Y-FW is grateful the University of Warwick and the EPSRC for financial support.

5. References

Ackermann Misfeldt, A., Costa, R. H., Gannon, M., 2008. β-cell proliferation, but not neogenesis, following 60% partial pancreatomy is impaired in the absence of FoxM1. Diabetes 57, 3069–3077.

Akirav, E., Kushner, J. A., Herold, K. C., 2008. β-cell mass and Type 1 diabetes. Diabetes 57, 2883–2888.

Beith, J. L., Alejandro, E. U., Johnson, J. D., 1998. Insulin stimulates primary β-cell proliferation via Raf-1 kinase. Endocrinology 149, 2251–2260.

Bonner-Weir, S., 2000. Perspective: Postnatal pancreatic β cell growth. Endocrinology 141, 1926–1928.

Bouwens, L., Rooman, I., 2005. Regulation of pancreatic beta-cell mass. Physiol. Rev. 85, 1255–1270.

Brook, C. G. D., Marshall, N. J., 2001. Essential Endocrinology. Blackwell Science.

De León, D. D., Deng, S., Madani, R., Ahima, R. S., Drucker, D. J., Stoffers, D. A., 2003. Role of endogenous glucagon-like peptide-1 in islet regeneration after partial pancreatectomy. Diabetes 52, 365–371.

De Winter, W., DeJongh, J., Post, T., Ploeger, B., Urquhart, R., Moules, I., Eckland, D., Danhof, M., 2006. A mechanism-based disease progression model for comparison of long-term effects of prioglitazone, metformin and gliclazide on disease processes underlying type 2 diabetes mellitus. J. Pharmacokin. Pharmacodyn. 33 (3), 313–343.

Dor, Y., Brown, J., Martinez, O. I., Melton, D. A., 2004. Adult pancreatic β-cells are formed by self-duplication rather than stem-cell differentiation. Nature 429, 41–46.

Efanova, I., Zaitsev, S., B., Z., Köhler, M., Efendić, S., Orrenius, S., Berggren, P. O., 1998. Glucose and tolbutamide induce apoptosis in pancreatic β-cells. A process dependent on intracellular Ca^{2+} concentration. J. Biol. Chem. 273, 33501–33507.

Frayn, K. N., 2003. Metabolic Regulation: A Human Perspective. W. B. Saunders.

Grossman, E. J., Lee, D. D., Tao, J., Wilson, R. A., Park, S.-Y., Bell, G. I., Chong, A. S., 2010. Glycemic control promotes pancreatic beta-cell regeneration in streptozotocin-induced diabetic mice. PLoS ONE 5, e8749.
URL doi:10.1371/journal.pone.0008749

Holmes, M. H., 1995. Introduction to Perturbation Methods. Springer.

Hope, K. M., Tran, P. O. T., Zhou, H., Oseid, E., Leroy, E., Robertson, R. P., 2004. Regulation of α-cell function by the β-cell in isolated human and rat islets deprived of glucose: the "switch-of" hypothesis. Diabetes 53, 1488–1495.

Imagawa, A., Hanafusa, T., Miyagawa, J.-I., Matsuzawa, Y., 2000. A novel subtype of type 1 diabetes mellitus characterized by a rapid onset and an absence of diabetes-related antibodies. N. Engl. J. Med. 342, 301–307.

Johnson, J. D., Alejandro, E. U., 2008. Control of pancreatic β-cell fate by insulin signaling: The sweet spot hypothesis. Cell Cycle 7, 1343–1347.

Johnson, J. D., Bernal-Mizrachi, E., Alejandro, E. U., Han, Z., Kalynyak, T. B., Li, H., Beith, J. L., Gross, J., Warnock, G. L., Townsend, R. R., Permutt, M. A., Polonsky, K. S., 2006. Insulin protects islets from apoptosis via Pdx1 and specific changes in the human islet proteome. Proc. Natl. Acad. Sci. USA 103, 19575–19580.

Jonas, J.-C., Laybutt, D. R., Steil, G. M., Trivedi, N., Pertusa, J. G., Van de Casteele, M., Weir, G. C., Henquin, J.-C., 2001. High glucose stimulates early response gene c-Myc expression in rat pancreatic cells. J. Biol. Chem. 276, 35375–35381.

Keener, J., Sneyd, J., 1998. Mathematical Physiology. Springer.

Lee, C. S., León, D. D. D., Kaestner, K. H., Stoffers, D. A., 2006. Regeneration of pancreatic islets after partial pancreatectomy in mice does not involve the reactivation of neurogenin-3. Diabetes 55, 269–272.

Lingohr, M. K., Buettner, R., Rhodes, C. J., 2002. Pancreatic β-cell growth and survival—a role in obesity-linked type 2 diabetes? TRENDS Mol. Med., 375–384.

Lipsett, M., Finegood, D. T., 2002. β-cell neogenesis during prolonged hyperglycemia in rats. Diabetes 51, 1834–1841.

Mentlein, R., Gallwitz, B., Schmidt, W. E., 1993. Dipeptidyl peptidase IV hydrolyses gastric inhibitory polypeptide, glucagon-like peptide-1(7-36)amide, peptide histidine methionine and is responsible for their degradation in human serum. Eur. J. Biochem. 214, 829–835.

Nielsen, J. H., Svensson, C., Galsgaard, E. D., Møldrup, A., Billestrup, N., 1999. Beta cell proliferation and growth factors. J. Mol. Med. 77, 62–66.

Nir, T., Melton, D. A., Dor, Y., 2007. Recovery from diabetes in mice by β cell regeneration. J. Clin. Invest. 117, 2553–2561.

Okada, T., Liew, C. W., Hu, J., Hinault, C., Michael, M. D., Krützfeldt, J., Yin, C., abd Markus Stoffel, M. H., Kulkarni, R. N., 2007. Insulin receptors in β-cells are critical for islet compensatory growth response to insulin resistance. Proc. Natl. Acad. Sci. USA 104, 8977–8892.

Pattaranit, R., van den Berg, H. A., 2008. Mathematical models of energy homeostasis. J. R. Soc. Interface 5, 1119–1135.

Pavliotis, G., Stuart, A., 2008. Multiscale Methods: Averaging and Homogenization. Springer.

Pelengaris, S., Khan, M., 2003. The many faces of c-Myc. Arch. Biochem. and Biophys. 416, 129–136.

Pelengaris, S., Khan, M., Evan, G. I., 2002. Suppression of Myc-induced apoptosis in β cells exposes multiple oncogenic properties of Myc and triggers carcinogenic progression. Cell 109, 321–334.

Protter, M. H., Morrey, C. B., 1970. College Calculus with Analytic Geometry. Addison-Wesley.

Raju, B., Cryer, P. E., 2005. Maintenance of the postabsorptive plasma glucose concentration: Insulin or insulin plus glucagon? Am. J. Physiol. Endocrinol. Metab. 289, E181–E186.

Ribbing, J., Hamrén, B., Svensson, M. K., Karlsson, M. O., 2010. A model for glucose, insulin, and beta-cell dynamics in subjects with insulin resistance and patients with Type 2 diabetes. J. Clin. Pharmacol. 50, 861–872.

Rooman, I., Lardon, J., Bouwens, L., 2002. Gastrin stimulates β-cell neogenesis and increases islet mass from transdifferentiated but not from normal exocrine pancreas tissue. Diabetes 51, 686–690.

Salway, J. G., 1999. Metabolism at a Glance. Blackwell Science.

Schmidt, R. F., Thews, G. (Eds.), 1989. Human Physiology, 2nd Edition. Springer.

Sofroniou, M., Spaletta, G., 2004. Construction of explicit Runge–Kutta pairs with stiffness detection. Math. Computer Modell. 40, 1157–1169.

Steil, G. M., Trivedi, N., Jonas, J.-C., Hasenkamp, W. M., Sharma, A., Bonner-Weir, S., Weir, G. C., 2001. Adaptation of β-cell mass to substrate oversupply: Enhanced function with normal gene expression. Am. J. Physiol. Endocrinol. Metab. 280, E788–E796.

Sturis, J., Polonsky, K. S., Mosekilde, E., Cauter, E. V., 1991. Computer model for mechanisms underlying ultradian oscillations of insulin and glucose. Am. J. Physiol. Endocrinol. Metab. 260, E801–E809.

Tolić, I. M., Mosekilde, E., Sturis, J., 2000. Modeling the insulin–glucose feedback system: The significance of pulsatile insulin secretion. J. Theor. Biol. 207, 361–375.

Topp, B., Promislow, K., Vries, G. D., Miura, R. M., Finegood, D. T., 2000. A model of β-cell mass, insulin, and glucose kinetics: Pathways to diabetes. J. Theor. Biol 206, 605 – 619.

Van de Casteele, M., Kefas, B. A., Cai, Y., Heimberg, H., Scott, D. K., Henquin, J. C., Pipeleers, D., Jonas, J, C., 2003. Prolonged culture in low glucose induces apoptosis of rat pancreatic β-cells through induction of c-myc. Biochem. Biophys. Res. Commun. 312, 937–944.

Watkins, P. J., 2003. ABC of Diabetes. BMJ Books.

Weir, G. C., Laybutt, D. R., Kaneto, H., Bonner-Weir, S., Sharma, A., 2001. β-cell adaptation and decompensation during the progression of diabetes. Diabetes, S154–S159.

Young, J., Pelengaris, S., Chipperfield, A., Heath, W. P., Khan, M., 2008. Engineering beta cell mass regulation in diabetes. Curr. Topics Biochem. Res. 10, 47–78.

Table 1: Notation and parameter values

Parameter	Value	Units	Interpretation
Φ	0.2	l min^{-1}	blood/interstitial space permeability
V_p	3	l	insulin distribution volume
V_i	11	l	interstitial space volume
V_g	10	l	glucose distribution volume
τ_g	6	min	mean lifetime of insulin in plasma
τ_i	100	min	mean lifetime of insulin in interstitial space
τ_d	36	min	response delay of glucose release
α_1	1.86	—	first sensitivity of β-cell death
α_2	14.5	—	second sensitivity of β-cell death
α_{II}	4.8	—	sensitivity of insulin-independent glucose uptake
α_{ID}	1.77	—	sensitivity of insulin-dependent glucose uptake
$\alpha_{\text{GR,i}}$	7.54	—	insulin sensitivity of hepatic glucose release
$\alpha_{\text{GR,g}}$	10	—	glucose sensitivity of hepatic glucose uptake
α_{IS}	6.67	—	sensitivity of insulin secretion
α_{GX}	0.00065	—	renal excretion parameter
$\alpha_{\text{NG,i}}$	0.5	—	sensitivity of neogenesis to insulin
$\alpha_{\text{NG,g}}$	0.5	—	sensitivity of neogenesis to glucose
γ_1	1.6	g l^{-1}	first pivot point of β-cell death rate
γ_2	2.6	g l^{-1}	second pivot point of β-cell death rate
$\gamma_{\text{II,lo}}$	144	mg l^{-1}	pivot point of non-splanchnic insulin-independent glucose uptake
$\gamma_{\text{II,hi}}$	2	g l^{-1}	pivot point of splanchnic insulin-independent glucose uptake
γ_{ID}	1	g l^{-1}	pivot point of insulin-dependent glucose uptake
γ_{GR}	2	g l^{-1}	pivot point of glucose release
γ_{IS}	2	g l^{-1}	pivot point of insulin secretion
γ_{GX}	0.3	g l^{-1}	renal excretion parameter
γ_{NG}	1.3	g l^{-1}	pivot point of neogenesis for glucose dependence
δ	0.34	—	contribution of non-splanchnic insulin-independent glucose uptake
δ_0	0.64	—	insulin-sensitive portion of β-cell proliferation
ι_0	115	mU l^{-1}	pivot point of β-cell proliferation rate
ι_{ID}	80	mU l^{-1}	pivot point of insulin-dependent glucose uptake
ι_{GR}	26	mU l^{-1}	pivot point of hepatic glucose release
ι_{AI}	0.3	U l^{-1}	pivot point for apoptosis inhibition
ι_{NG}	30	mU l^{-1}	pivot point for neogenesis for insulin dependence
ψ_0	40	mg min^{-1}	baseline of insulin-dependent glucose uptake
$\widehat{\psi}_{\text{II}}$	0.21	g min^{-1}	maximum flux: insulin-independent glucose uptake
$\widehat{\psi}_{\text{ID}}$	0.94	g min^{-1}	maximum flux: insulin-dependent glucose uptake
$\widehat{\psi}_{\text{GR}}$	0.18	g min^{-1}	maximum flux: hepatic glucose release
$\widehat{\psi}_{\text{IS}}$	0.21	U min^{-1}	maximum flux: insulin secretion
$\widehat{\psi}_{\text{NG}}$	0.001	min^{-1}	maximum flux: neogenesis of β-cell mass
ψ^*_{GX}	29	mg min^{-1}	renal excretion parameter
ρ_0	0.166	year^{-1}	baseline β-cell proliferation rate
$\widehat{\mu}$	0.311	year^{-1}	maximum β-cell death rate

The term "pivot point" refers to midrange values, saturation constants etc. of saturating responses.
Insulin units: 1 U $\doteq$ 6.67 nmol.

Appendix A. Functional relationships for rates and fluxes

The ψs are fluxes and rates modelled by empirical functions: ψ_{II} represents insulin-independent glucose uptake by body cells:

$$\psi_{\text{II}}(G) = \widehat{\psi}_{\text{II}} \left[\delta \left(1 - \exp\left\{ -\frac{G/V_g}{\gamma_{\text{II,lo}}} \right\} \right) + \frac{1-\delta}{1 + \exp\left\{ \alpha_{\text{II}} \left(1 - \frac{G/V_g}{\gamma_{\text{II,hi}}} \right) \right\}} \right] \tag{A.1}$$

where $\widehat{\psi}_{\text{II}}$, $\gamma_{\text{II,lo}}$, $\gamma_{\text{II,hi}}$, δ, and V_g are positive parameters (see Table 1 for values). Insulin-dependent glucose uptake is represented by ψ_{ID}:

$$\psi_{\text{ID}}(G) = \frac{G/V_g}{\gamma_{\text{ID}}} \left[\psi_0 + \frac{\widehat{\psi}_{\text{ID}} - \psi_0}{1 + \exp\left\{ -\alpha_{\text{ID}} \ln\left\{ (I_i/\iota_{\text{ID}})({V_i}^{-1} + (\Phi\tau_i)^{-1}) \right\} \right\}} \right] \tag{A.2}$$

with positive parameters ψ_0, $\widehat{\psi}_{\text{ID}}$, α_{ID} γ_{ID}, and ι_{ID}. Endogenous release of glucose is represented by ψ_{GR}:

$$\psi_{\text{GR}}(G, w_3) = \widehat{\psi}_{\text{GR}} \left(1 + \exp\left\{ -\alpha_{\text{GR,g}} \left(1 - \frac{G/V_g}{\gamma_{\text{GR}}} \right) \right\} \right)^{-1} \left(1 + \exp\left\{ -\alpha_{\text{GR,i}} \left(1 - \frac{w_3/V_p}{\iota_{\text{GR}}} \right) \right\} \right)^{-1} \tag{A.3}$$

with positive parameters $\widehat{\psi}_{\text{GR}}$, $\alpha_{\text{GR,i}}$, $\alpha_{\text{GR,g}}$, ι_{GR}, and γ_{GR}. Insulin secretion from pancreatic β-cells is represented by ψ_{IS}:

$$\psi_{\text{IS}}(G) = \widehat{\psi}_{\text{IS}} \left(1 + \exp\left\{ \alpha_{\text{IS}} \left(1 - \frac{G/V_g}{\gamma_{\text{IS}}} \right) \right\} \right)^{-1} \tag{A.4}$$

with positive parameters $\widehat{\psi}_{\text{IS}}$, α_{IS}, and γ_{IS}. Renal excretion of glucose, which becomes important at elevated glucose levels, is represented by ψ_{GX}:

$$\psi_{\text{GX}} = \psi^*_{\text{GX}} \ln\left\{ 1 + \alpha_{\text{GX}} \exp\left\{ \frac{G/V_g}{\gamma_{\text{GX}}} \right\} \right\} \tag{A.5}$$

with positive parameters ψ^*_{GX}, α_{GX}, and γ_{GX}. The proliferation rate of the β-cells is assumed to be dependent on the insulin concentration:

$$\rho(I_p) = \rho_0 \left(1 + \delta_0 \frac{I_p}{\iota_0 V_p + I_p} \right) \tag{A.6}$$

with positive parameters ρ_0, α_0, and ι_0. The death rate of the β-cells is assumed to be dependent on the glucose concentration and the interstitial insulin concentration:

$$\mu(G, I_i) = \widehat{\mu} \left(1 + \frac{I_i/V_i}{\iota_{\text{AI}}} \right) \left(1 + \exp\left\{ \alpha_1 - \frac{G/V_g}{\gamma_1} - \alpha_2 \left(1 - \frac{G/V_g}{\gamma_2} \right)^4 \right\} \right)^{-1} \tag{A.7}$$

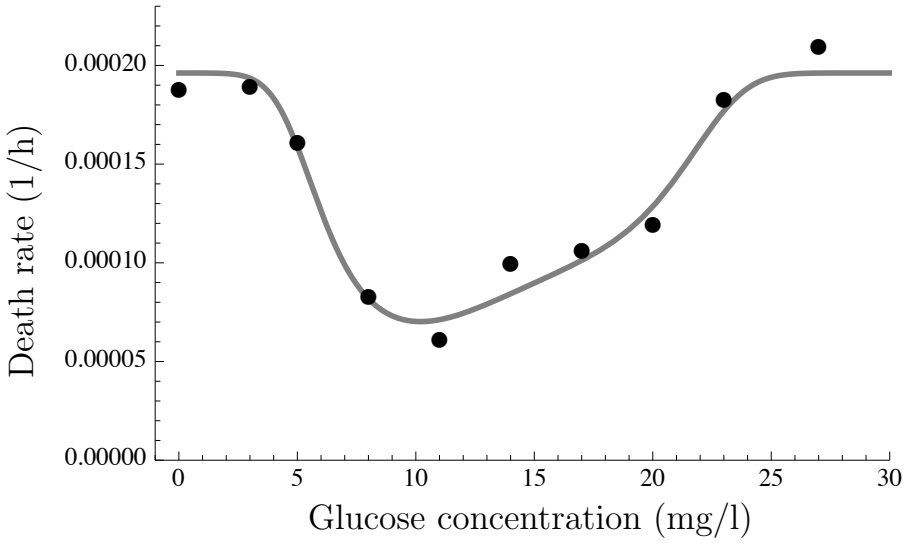

Figure B.8: Pancreatic β-cell death rate data and least-squares fit of the formula used in the model.

with positive parameters $\widehat{\mu}$, α_1, α_2, γ_1, and γ_2. The above formulas and the values listed in Table 1 have been taken from Tolić et al. (2000), with the addition of two novel elements: glucose excretion (ψ_{GX}), which is necessary to represent hyperglycaemic challenges, and the β-cell mass dynamics. Glucose excretion is based on the graph given in Schmidt and Thews (1989), whereas β-cell mass dynamics is based on various data from the literature, as detailed in Appendix B.

Appendix B. Parameter estimation for β-cell dynamics

Whereas the fast time-scale parameters could be adopted from Tolić et al. (2000), the rates of proliferation, death, and neogenesis of β-cells had to be estimated from the experimental literature. Although the model describes the human system, the parameter values here are taken from experiments on rodents, which is a limitation. However, the parameters represent cellular characteristics which may to a first approximation be assumed to be transferrable from the rodent to the human setting. An exception is the parameter $\widehat{\psi}_{\text{NG}}$, but our method of estimating this parameter implicitly contains the required scaling.

Appendix B.1. Death

Efanova et al. (1998) reported fractions of surviving β-cells after 40 hours and exposure to varying levels of glucose. The average death rate per hour over this interval can be estimated using the formula $-\ln\{f\}/(40\text{ hrs})$ where f is the fraction cells alive after 40 hrs of exposure. Death rates thus obtained are plotted as a function of the ambient glucose concentration in Fig. B.8. Equation (A.7), which is not intended as a mechanistic explanation but merely to capture the phenomenology, was fitted to these data by non-linear least-squares. However, it was found that these rates were several orders of magnitude larger than the accepted β-cell turn-over rate quoted

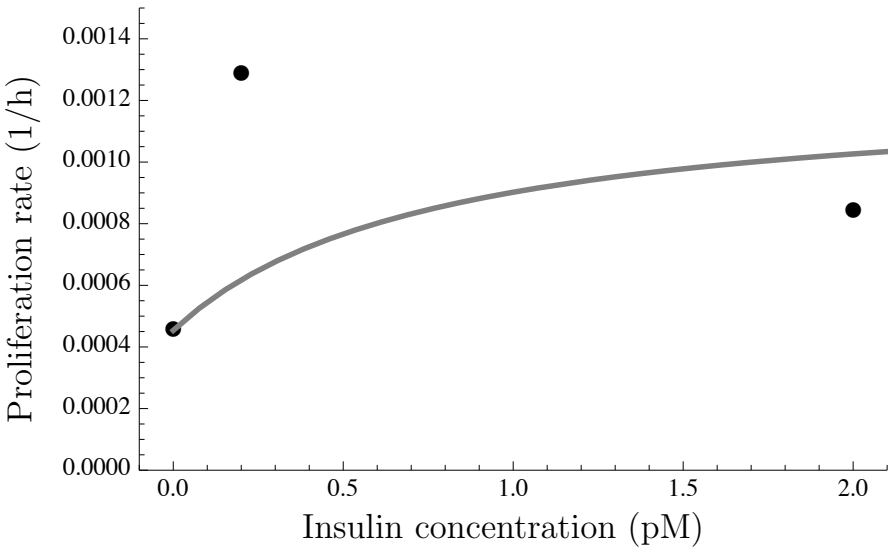

Figure B.9: Pancreatic β-cell proliferation rate data and least-squares fit of the hyperbolic formula used in the model.

in the literature (Dor et al., 2004; Topp et al., 2000), a fact we attributed to the unfavourable *ex vivo* conditions under which these data were obtained. For this reason, we scaled the parameter $\widehat{\mu}$ in such a way that the standard cycle described in the main text would be characterised by a balance of β-cell birth and death.

Johnson et al. (2006) documented a direct anti-apoptotic effect of insulin, quantified by various measures which showed broadly similar trends in dependence upon insulin concentration, the effect being most pronounced at low insulin levels and diminishing hyperbolically as insulin is increased to hyper-physiological levels. Johnson and Alejandro (2008) synthesised these trends in a single graph, which shows that the relative potency of the anti-apoptotic effect drops off more or less hyperbolically with insulin concentration I, i.e. as follows:

$$\text{relative effect} = \frac{1}{\iota_{\text{AI}} + I} \tag{B.1}$$

where ι_{AI} is approximately 0.3 U l^{-1}. The reciprocal of this protective effect appears as a prefactor of the death rate in equation (A.7).

Appendix B.2. Proliferation

Okada et al. (2007) and Beith et al. (1998) demonstrated that insulin stimulates β-cell proliferation. Data taken from the latter paper were used to fit a simple hyperbolic model, equation (A.6), shown in Figure B.9.

Appendix B.3. Neogenesis

Neogenesis of β-cells remains to be fully characterised in quantitative terms. The formula used in this paper to represent the rate at which β-cells are replenished is therefore speculative. To

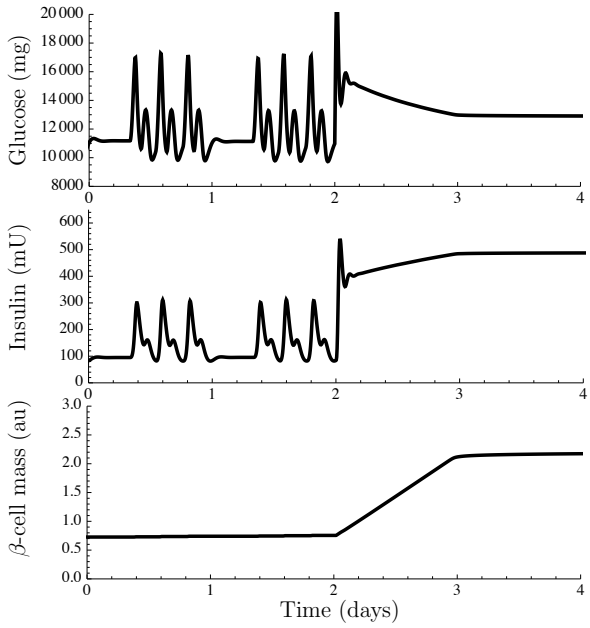

Figure B.10: The Steil et al. experiment as simulated by the present model. After two control days, glucose is switched to an infusion. Top: plasma glucose content; middle: interstitial space insulin content; bottom: β-cell mass.

obtain reasonable values for the relevant parameters (those with subscript NG), simulations were performed that mimicked an experiment described by Steil et al. (2001) in which rats were given infusions of glucose that initially doubled the plasma glucose levels. Within a day, euglycemia was re-established and the β-cell mass had doubled. The simulations are shown in Figure B.10